HORIZON 2020

Research Infrastructures

H2020-INFRAIA-2014-2015

INFRAIA-1-2014-2015 Integrating and opening existing national and regional research infrastructures of European interest

ENSAR2

European Nuclear Science and Application Research 2

Grant Agreement Number: 654002

D10.5 Final Report on the New technologies on passivation and segmentation and R&D on novel Ge-detector geometries for ultimate position resolution and efficiency

Version: 1.0
Author: D.Napoli, J.Gerl
Date: 28/02/2020

PROJECT AND DELIVERABLE INFORMATION SHEET

ENSAR2 Project Ref. №	654002
Project Title	European Nuclear Science and Application Research 2
Project Web Site	http://www.ensarfp7.eu/
Deliverable ID	D10.5
Deliverable Nature	Final Report
Deliverable Level*	PU
Contractual Date of Delivery	February 29th 2020
Actual Date of Delivery	February 28th 2020
EC Project Officer	René Martin

* The dissemination level are indicated as follows: PU – Public, PP – Restricted to other participants (including the Commission Services), RE – Restricted to a group specified by the consortium (including the Commission Services). CO – Confidential, only for members of the consortium (including the Commission Services).

DOCUMENT CONTROL SHEET

Document	Title: Final Report on the New technologies on passivation and segmentation and R&D on novel Ge-detector geometries for ultimate position resolution and efficiency	
	ID: D10.5	
	Version 0.0	
	Available at: http://www.ensarfp7.eu/	
	Software Tool: Microsoft Office Word 2007	
	File:	
Authorship	Written by:	D.Napoli, J.Gerl
	Contributors:	
	Reviewed by:	N. Marginean, IFIN HH
	Approved by:	M. N. Harakeh, KVI Cart

DOCUMENT STATUS SHEET

Version	Date	Status	Comments
0.1	19/02/2020	For internal review	
1.0	27/02/2020	For internal review	
1.0	28/02/2020	Submitted on EC Participant Portal	
		Final version	

DOCUMENT KEYWORDS

Keywords	Position sensitive Germanium detectors, Imaging techniques, HP-Ge Detector associated techniques

Disclaimer

This deliverable has been prepared by Work Package 10 (PSeGe) of the Project in accordance with the Consortium Agreement and the Grant Agreement n°654002. It solely reflects the opinion of the parties to such agreements on a collective basis in the context of the Project and to the extent foreseen in such agreements.

Copyright notices

TABLE OF CONTENTS

LIST OF FIGURES

Figure 1.E.2 shows the spectra of ^{241}Am and ^{133}Ba up to 400 keV for both segments. Higher energies have very low efficiency because the reduce thickness of the detector (2mm). The gap in between segments is 0,4 mm.

Figure 1.E.3: Both figures compare the signal shapes generated by COMSOL (red line) obtained in the modelling described in the precedent section 1.D with the real signals obtained with the segmented detector described in section 1B.

Figure 1.F.1: From top to bottom, bulk potential and field lines at increasing surface charge density.

Figure 2.1: Quasi-planar prototype p-type HPGe detector with dimensions of 33.2x33.2x15.5 mm3 used in order to determine the energy resolution of such a system with a single point contact read out. The depletion voltage was calculated as 450V.

Figure 2.2: Semi-planar crystal placed in a POPTOP type capsule. The assembly and front-end electronics is shown.

Figure 2.3: The observed energy spectrum with 57Co source. The spectrum on the left side was recorded using a 6 µs shaping time constant while the one on the right side was obtained with a 3 µs shaping time constant.

Table 2.1: Energy resolution values obtained with a semi-planar point-contact detector listed for ^{57}Co and ^{60}Co transitions, using different shaping time constants.

Figure 2.4: Different kind of couplings were used in order to read the signal at GSI and SEMIKON. Left drawing illustrates the DC coupling used at GSI and the left drawing shows the AC coupling used by SEMIKON.

Figure 2.5: Schematics of the GSI scanner and the actual measurement set-up.

Figure 2.6: Images of the front (a, c) and side (b, d) scan.

Figure 2.7: Multitudes of line shapes for the side and front scan of the Quasiplanar detector.

REFERENCES AND APPLICABLE DOCUMENTS

[1] J. Eberth, J. Simpson, Prog. Part. Nucl. Phys. 60, 283 (2008).
[2] K. Vetter, Annu. Rev. Nucl. Part. Sci. 57, 363 (2007).
[3] C. Fleischmann et al., J. Mater. Chem. C 1, 4105 (2013).
[4] P.W. Loscutoff, S.F. Bent, Annu. Rev. Phys. Chem. 57, 467 (2006).
[5] G.W. Anderson et al., Appl. Phys. Lett. 66, 1123 (1995).
[6] S. Rivillon et al., Appl. Phys. Lett. 87, 253101 (2005).
[7] T. Maeda et al., J. Appl. Phys. 100, 014101 (2006).
[8] D. Bodlaki et al., Surf. Sci. 543, 63 (2003).
[9] K. Park, Y. Lee, S. Lim, Appl. Surf. Sci. 254, 1842 (2008).
[10] G. Maggioni et al., Eur. Phys. J. A (2015) 51: 141.
[11] CTT Cryostat and Detector Technique Thomas, Montabaur, Germany
[12] COMSOL Multiphysics, a cross-platform finite element analysis, solver and multiphysics simulation software (see https://www.comsol.com/)
[13] Semikon Detector GmbH, Jülich, Germany
[14] Zhong He, Nucl. Instr. and Meth. in Phys. Res. A 463 (2001) 250
https://doi.org/10.1016/S0168-9002(01)00223-6

LIST OF ACRONYMS AND ABBREVIATIONS

COMSOL	**COMSOL Multiphysics** is a cross-platform finite element analysis, solver and multiphysics simulation software (see https://www.comsol.com/)

HPGe	High Purity Germanium
CTT Company	CTT Cryostat and Detector Technique Thomas, Montabaur, Germany
SEMIKON	Semikon Detector GmbH, Jülich, Germany
FET	Field-effect transistor
PSA	Pulse-shape analysis

EXECUTIVE SUMMARY

This report includes the results of two task within Work package 10. The first task aimed to develop Technological improvements on the production of segmented coaxial detectors, with newly passivation and segmentation technologies. Several hydride passivating treatments tested with detector prototypes. Newly technologies for contact segmentation have been developed.

Regarding the second task, developments on semi-planar detector with point contacts have been performed at GSI at the level of prototype. Performance measurements and characterization scanning of the prototype have been completed. Reduced non-active volume has been found, in agreement with calculations.

INTRODUCTION

High-purity germanium (HPGe) detectors are still the most important instruments for high-resolution gamma-ray spectroscopy [1, 2]. An HPGe detector is a diode produced from an extremely pure Ge single crystal with a net impurity concentration around 10^{10} atoms cm^{-3}. The n and p contacts of the diode are placed on the opposite sides of the Ge crystal and are reverse biased in order to achieve the complete charge depletion of the Ge crystal volume. Because of the gamma ray interaction with the detector, electrical charges are created and collected to the contacts. The intrinsic surface between the n and p contacts of an HPGe detector is the most critical part and must be passivated in order to remove electronic states in the Ge band gap (electrical passivation) and to prevent the surface from reacting with the atmosphere (chemical passivation) [3].

The technology used for the production of standard coaxial detectors is well established and reliable, but the situation is quite different for the new generation of highly segmented detectors for gamma tracking. We are reporting here on the results obtained in two tasks, which have addressed the problem of segmented detectors for gamma tracking from different points of view:
- The first of these tasks have looked for new technologies on passivation and segmentation.
- The second one have studied novel HPGe geometries proposing a new approach to the problem. A proof of concept of a new geometry has been constructed in the collaboration of a private company.

One of the most serious issues in the fabrication of Ge devices concerns the passivation of Ge surfaces. Differently from Si, Ge forms unstable oxides: GeO2 is water-soluble and decomposes under thermal treatment around 420◦C [3] so that it cannot be used in wet processes and thermal treatments in ULSI fabrication processes [4]. For this reason, alternative passivation coatings have been studied and developed and several Ge-based dielectric com-pounds (such as Ge nitrides and oxynitrides) are now considered potentially interesting for technological applications. In particular, germanium nitride (Ge3N4) exhibits a high dielectric constant, is water-insoluble and its thermal decomposition temperature is higher than GeO2 [5,6] so that it could be applied not only as a buffer layer for high-k dielectrics grown on Ge substrates but also for the passivation of Ge surfaces. Germanium oxynitrides (GeOxNy) are also promising materials, because nitrogen incorporation in GeO2 has proven to improve its chemical and thermal stability [7]: the decomposition temperature of a GeOxNy layer was found to increase up to 550◦C, which was more than 100◦C higher than that of pure GeO2 [8,9].

An extensive work on passivation of HPGe surfaces for detectors has been done and published under the 7th Framework Program FP7/2007-2013, under grant agreement No. 262010 - ENSAR-INDESYS [10] and the present task has obtained an important improvement of those technologies that have been applied also to the passivation of the gap in between segments.

As shown in our precedent publication, careful 2D scans of the full Ge at a 2-mm pitch and simulations are fundamental for properly determining the charge collection and deduce the electric field in the prototype crystals in order to quantify the benefit of the different surface-treatment techniques tested. Detailed studies in selected parts of the crystal volume can be also performed with much better spatial resolution down to 0.5 mm.

Then, the goals of the first task include R&D of segmented contacts in HPGe detectors and of the passivation of the boundary regions between contacts, charge collection and electric-field exploration via 2D scans. This first task has been completed mainly at the Materials Physics Laboratory of the INFN by a multidisciplinary group with members from INFN and the Physics and Astronomy Department of the University of Padova, composed by nuclear and solid state physicists, chemists and material engineers. Some surface analyses have been also done at the University of Padova, simulations have been performed at CSIC and Padova and the surfaces scanning runs have been done with the support and experience of the INFN and IPHC groups, this last with a long tradition and exceptional equipment for these purposes. For the tests of the detectors, IKP and INFN have designed a new cryostat that has been built by the CTT Company [11].

The second task R&D on novel Ge-detector geometries for ultimate position resolution and efficiency (GSI) In “planar” detectors with high position resolution, the detector geometry design and contacts are still an issue. The structure of the detector requires a guard ring forming a dead region, which uses about 20% of the Ge volume. The high position resolution of a planar Ge detector is important for future arrays with imaging capabilities as well as for the applications based on gamma-ray imaging.

The aim of this task was to develop a prototype of a 3D position-sensitive Ge gamma-detector with 1-2 mm position resolution and maximal active/total volume ratio by using a novel contact technologies proposed for planar and quasi-planar “point contact” detectors. This development have included the modelling and simulation of electrical-field distributions aiming to maximise the active volume, the evaluation of the 3D position resolution obtainable, the production of a prototype detector in cooperation with the industrial partner SEMIKON [13] and the experimental tests for the characterization of the detector and the determination of the position resolution. For this purpose, 3D scanning of the volume have been done.

SECTION 1 - NEW TECHNOLOGIES ON PASSIVATION AND SEGMENTATION (INFN, IKP, IPHC/CNRS, CSIC)

1.A. NEW PASSIVATION FOR HPGE DETECTORS

At the INFN’s National Laboratories of Legnaro a specific program for the production of HPGe detector prototypes with novel technologies is currently running. As shown in a precedent work, several passivation treatments have been applied and characterized as for both their composition and structure and their performances as passivation layers [10].

Now we are reporting here the most recent results of a new Ge-hydride termination that shows still better characteristics than previously reported passivations obtained with H-termination chemical methods, in particular for key features such as depletion voltage, leakage currents, etc.

The detector used for this study is the same that has been also used in ref. [10]. It is a planar n-type HPGe detector (cylindrical shape: 21 mm height, 39 mm diameter) with a contact of implanted B in one of the faces and a diffused Li contact on the opposite side. A circular gold electrode of 36 mm diameter was deposited on the B-implanted face so that the junction has to be considered of the diameter of the contact. The choice of working with the same detector for all the passivations is crucial to have a solid reference base for its bulk properties and

allows to compare in a straightforward way the results of all the different chemical treatments applied to it, being assured that only the passivation of the surface is changed.

After each passivation of the lateral surface, the detector was mounted in the customized support already shown in our reference [10].

We are comparing here the results obtained for the new passivation with other two hydride passivations studied in our precedent work [10]. The three passivations we are comparing here are different because of varying hydrofluoric acid (HF, semiconductor grade) concentration or the surface preparation procedures:
- Low concentration acid (labelled as Low H in our precedent work [10]):
- High concentration acid (High H in our precedent work [10]);
- The new procedure we are reporting here, called Hyper.

The properties of all three passivations have been tested by applying them to the same HPGe crystal as described in our reference [10] in both configurations described schematically in Figure 1.A.1 for characterizing the bulk and surface properties of the resulting detectors.

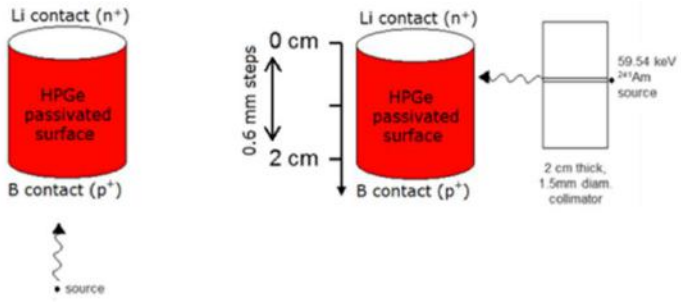

Figure 1.A.1: Two different types of measurements: the whole detector properties determination, putting the radiation source in front of the HPGe (on the left); the passivated surface study, putting the low-energy radiation source on the side of the HPGe (on the right).

The bulk properties of the HPGe detector obtained in this work with the so called Hyper H passivation are quite similar to those obtained in [10] for the Low H and High H passivations. The increasing of the counting rate in Hyper H as a function of the applied voltage, reaches the same plateau (maximum counting rate) than for the other two detectors but at a slightly higher voltage (1900 V instead of 1500 V) as can be seen in Figure 1.A.2.

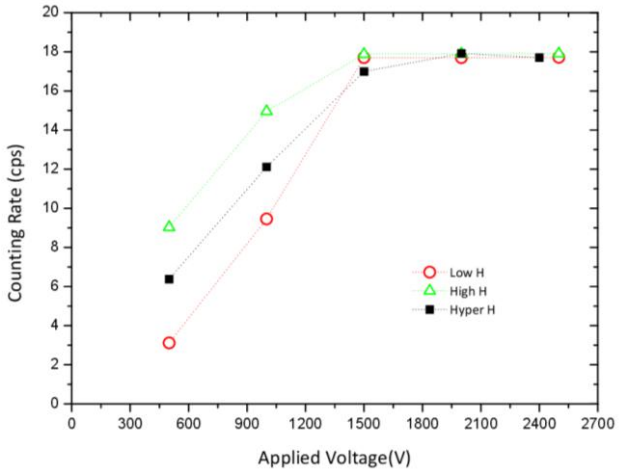

Figure 1.A.2: Counting rate of the 1.33 MeV ^{60}Co peak as a function of the applied voltage.

We can figure out, following the reference [10], that while the voltage is increasing, the depletion region extends accordingly going in two different directions: along the crystal thickness, from the p-n junction to the other contact, and transversally toward the lateral surfaces affected by both the bulk impurity concentration and the field distortions due to the electrical nature of eventual surface states created along the passivated surface. Since for the two previous treatments (Low H and High H) almost the same depletion voltage (Vd) has been observed, it can be inferred that a similar electrical nature of the surface states has been achieved even if the surface charge densities due to the chemical bonds could not be the same. For the new treatment, the Vd value necessary to reach the plateau is higher because the counting rate in the active volume can continue increasing at increasing voltages: this is due to the increase of the local electric field near the passivated surface, which leads to an improvement in the charge collection.

On the other hand, the counting rate at the plateau is almost the same for the three methods. This value depends on the active volume, whose differences are given by the dead layer below the intrinsic surface, since the contacts and the bulk crystal are similar, then, the average dead layer for the three methods would have to be similar.

As can be seen in Figure 1.A.3, the best resolution is nearly the same and at the same voltage (1500V) for the three methods but for the new passivation, the resolution essentially maintains its good value also at higher voltages that reflects a better collection of charges we have been referring above and that we will study in the detailed scanning of the surface.

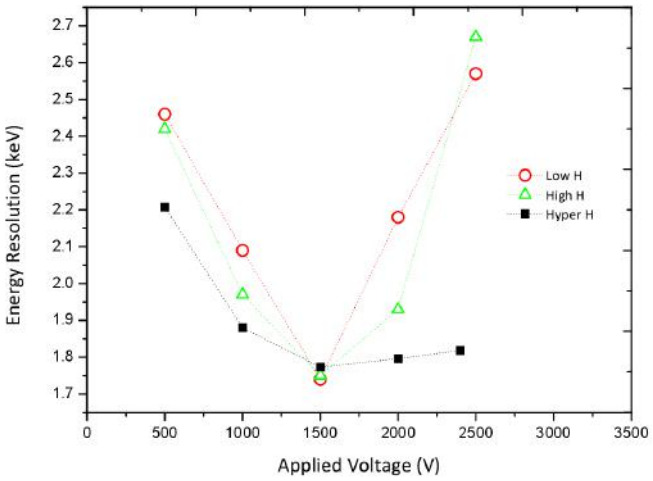

Figure 1.A.3. Energy resolution of the 1.33MeV 60Co peak as a function of the applied voltage.

As has been shown in [10] the measurement of the efficiency with different calibration sources (^{241}Am, ^{60}Co and ^{152}Eu) is not so sensitive to small differences in the passivation surfaces.

Most of the information is achieved by measuring the counting rate as a function of the distance of the contacts (every 0,6 mm). Both the passivations for the Low H and High H detectors have been published in reference [10] whereas Hyper H has been developed and studied in the present activity. All three scanning results, that can be seen in the Figure 1.A.4, have been done with the same bulk crystal and at 1500 V.

The counting rate (photopeak integral normalized by the acquisition live time) as a function of the distance between the source and the contacts has also investigated for each studied passivation treatment at different

applied voltages, moving always the collimated source from the Li contact (corresponding to distance d=0 in the plots) to the B one. As described in the ref. [10], we have only analyzed the spectra taken at more than 1,5 mm from the contacts because of the decreasing of the counting rate near the contacts due to the source illuminating cone and the contact dead layers.

By observing the trends of the counting rates for the different passivations, it is possible to gain information about the electrical nature of the surfaces. In spite of their very similar bulk properties, each H-termination has shown a different behavior for the lateral surface [Figure 1.A.4].

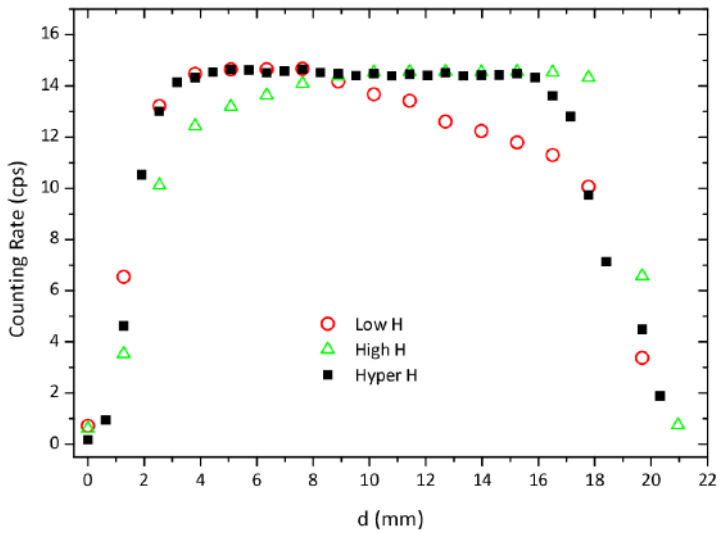

Figure 1.A.4: Counting rate of the 59.54keV ^{241}Am peak as a function of the distance of the source from the Li contact for the different passivations at 1500 V.

To schematize the different trends, we observe that:
- the counting rate for Low H passivation decreases moving from the n+ to p+ contact, giving rise to a slightly n-type surface;
- the counting rate for High H passivation increases from n+ to p+ contact, giving rise to a slightly p-type surface;
- the counting rate for Hyper H passivation remains constant along all the scan, giving rise to an almost ideal passivation.

For a better understanding it must be pointed out that the signals coming out from the detector are given by the sum of the contributions of electron and hole collection and so they depend on the interaction position since the electrons drift to be collected in the n+ contact while the holes go to the p+ contact. Therefore taking as example the Low H passivation case, on can infer that: the lower counting rate near the p+ contact could be related to a n^+-like behavior of the passivated surface which is reducing (or retarding outside the electronic window) the effective charge collection in the contacts. Then, the surface residual charge could produce a recombination of the charges or a delay in the transport to the contacts with the consequence that the detected energy will be lower and contribute to the spectra background instead of increasing the photo-peak area.

For applying these passivations to segmented contacts, we have developed the segmentation procedure at INFN as described below. For simplicity, for many tests necessary for learning about other processes (like segmentation, for example), we prefer to use the passivation created with methanol quenching (described in [10]).

1.B. SEGMENTATION PROCEDURE

We decided to test the segmentation by using lithography and etching to open insulating tracks over a continuous junction previously produced on the crystal. In order to tested different segmentation parameters we have developed an in house photolithography process for HPGe. This is a well-known technology for performing the segmentation of contacts in semiconductors but needs some shrewdness when applied to HPGe detectors for avoiding contaminations of the crystal in the processes. In fact, only few companies sell segmented HPGe detectors in the world.
For most of our developments we have used small planar HPGe 1 x 1 x 0,2 cm^3 crystals and we will describe the process for segmenting a single side planar detector. Before starting the segmentation processes, is necessary to create both continuous contacts in the planar detector. The segmentation by photolithography can be done only if the contact is very thin (few hundreds of nm).

Before starting the photolithography process the crystal has to be properly cleaned with an appropriated etching. Then we deposit a gold thin layer on the contact to be segmented which has the purpose of acting as a mask during the last crystal etching at the end of the process. Then, after the gold thin layer we start the sequence illustrated in Figure 1.B.1.

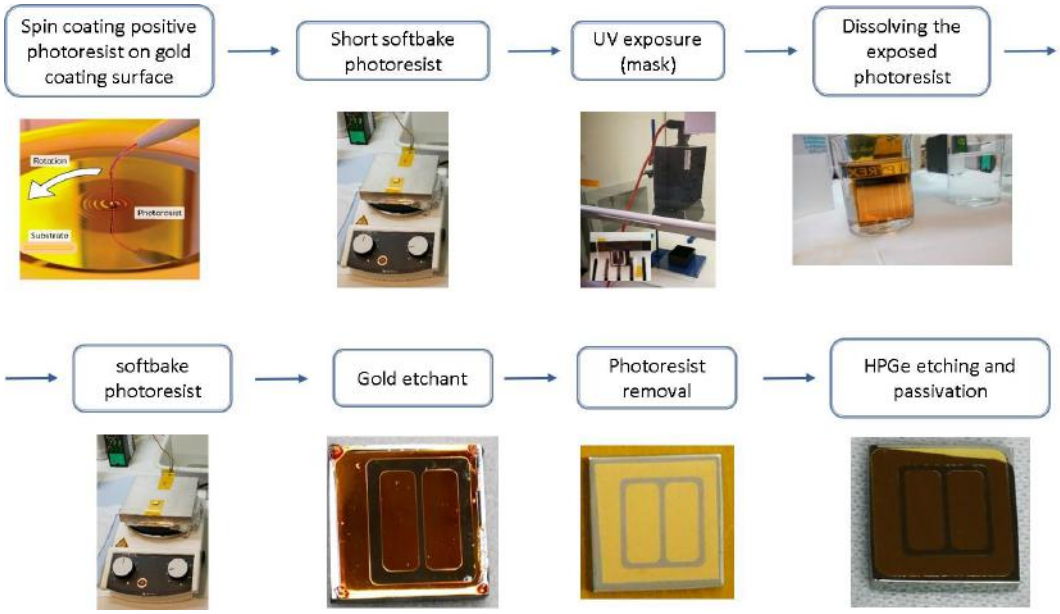

Figure 1.B.1. The photolithography process illustrated in our lab.

As can be noted in Figure 1.B.2 the contacts are well defined as a result of the procedure. In order to avoid possible tip effects when applying voltage, we decided to make rounded edges of both the contacts and the guard ring. Even the round parts of the drawing are properly implemented as can be seen by Scanning Electron Microscopy detail in Figure 1.B.2 right.

Figure 1.B.2: Photography of the segmented detector (left) and detail of the border of the segment observed by Scanning Electron Microscopy (right).

For the characterization tests as a diode (I-V plot) and as a detector through the acquisition of spectrum of calibration gamma sources, a new cryostat has been designed and constructed *ad hoc* with internal variable geometry, vacuum signal feedthroughs and preamplifiers for acquiring enough number of signals, that will be described in the next section (1.C).

1.C. Design and Construction of a Test Cryostat

The group at the INFN Legnaro, the Nuclear Physics Institute of the University of Cologne and the company Cryostat and Detector Technique Thomas Company (CTT [11]) developed together a test cryostat called SN10061 for measurements with prototype HPGe detectors. The CTT test cryostat system and its upgrade was optimized for R&D work on HPGe-Detectors. The cryostat is operated with a small dewar vessel for liquid nitrogen cooling enabling thereby the use of the system in any position in a close experimental setup e.g. within a scanning table. Therefore, the entire layout was designed to be small, thin and transparent for gamma radiation at low energies of several tenth of keV as possible. The cryostat is equipped with electronics for one central contact signal read out and up to twelve segment signal read outs. A group of six segments can be operated as n-type or p-type contacts, respectively. The first pre-amplifier feedback stages are operated with cold field effect transistor FET technology at liquid nitrogen temperature in high vacuum to optimize and to characterize the performance measurements of new detector techniques. Cold FET technology is typically not available for standard commercial HPGe detector cryostats. It allows for improved and refined measurement results due to noise reduction. The cryostat is equipped with additional feed-throughs enabling the measurement of the high resistivity of the diode characteristics of the new detectors without the necessity of a new assembly intervention. The electronics operated under standard atmospheric conditions are equipped with pre-amplifiers, which can be exchanged easily by a kind of “plug in - plug out” technology. The cryostat has in contrast to standard detector cryostats two high voltage feedthroughs allowing future designs with various HV levels e.g. for Ge strip detectors or other detector configurations.

1.D. Modelization of Segmentation

During the determination of the interaction position through the pulse shape analysis (PSA), we are nowadays using a database of calculated pulses for the comparison with the experimental ones. Equally, understanding the signals, provided by our detector prototype, requires a model with all the ingredients, like the charges mobility, but also more complex phenomena in the transportation of the charges between the interaction point and the contact. The complexity of the fields, especially in the boundary regions of the detector or in the vicinity of the segmentation areas, requires Monte-Carlo simulations with a complex field modelling software.

For studying the dynamics of the charge collection inside the HPGe detector it has been used COMSOL Multiphysics, a commercial software for simulating physical systems. This modelling performed at CSIC and INFN

has been used for illustrating the effects on the field inside the detector of the eventual presence of residual charges in the passivated surface.

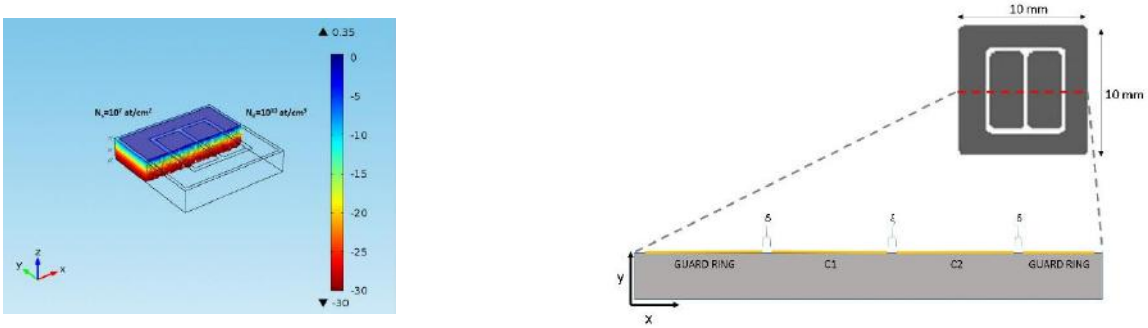

Figure 1.D.1: The Electrostatic Model environment was selected for the simulation of the potential distribution induced by the bias voltage on the non-segmented side (left) and for the calculations of the weighting potentials useful to compute the signals. The geometry (right) is similar to the real detector shown in Figure 1.B.2.

The geometry of the detector used for the COMSOL Modelling is shown in Figure 1.D.1 and it is similar to the real detector shown in Figure 1.B.2, in order to compare with the experimental results obtained in the laboratory. The Electrostatic Model environment was selected for the simulation of the potential distribution induced by the bias voltage on the non-segmented side and for the calculations of the weighting potentials useful to compute the signals. It is important to notice that the contacts developed in Task 3 are so thin (less than 300 nm) in relation with the detector thickness (2 mm) that their thickness can be neglected. A residual doping $N_b = 10^{10}$ cm^{-3} has been considered for the p-type bulk HPGe volume.

In Figure 1.D.2 central section of the segmented detector is represented (the position of the cut is shown with a dashed red line in the upper part of the figure). In the figure, the mash of the calculation is reported. Moreover in the upper part, the two contacts and the two guard-ring sectors are evidenced. All of them are at ground potential in the experiment and in the calculation and the gaps between them have been passivated. In order to better compute the charge dynamics at the border, we created a more dense mesh close to the three upper gaps. At the bottom we applied the boundary conditions for the polarization voltage considering a full continuous contact at negative voltage V= -25 V, where the full depletion occurs.

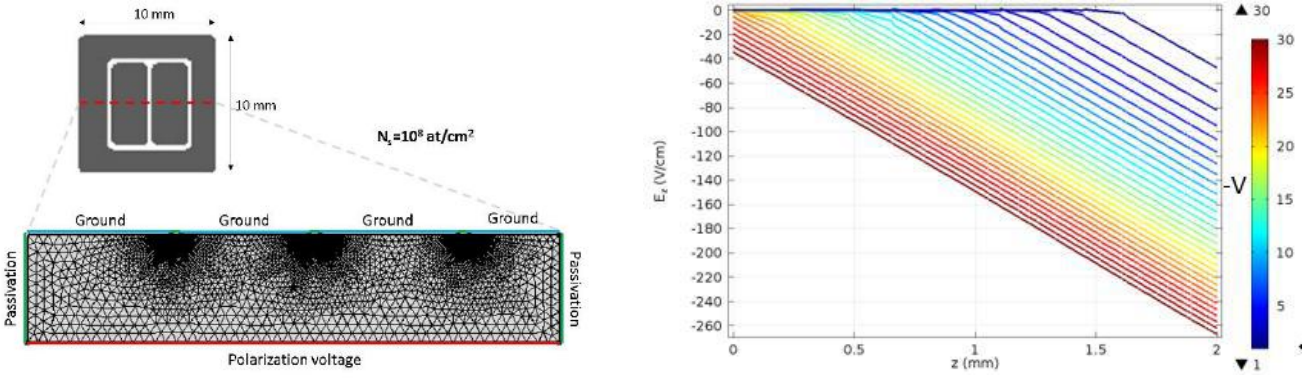

Figure 1.D.2: On the left part, the basic geometry of the segmented contacts is shown; the red dashed line indicates the section cut shown at the bottom. The segmented contacts and the two guard ring sections referenced at ground are evidenced with light blue lines. The passivated gaps and both lateral passivated surfaces are drawn in green while the ions and the full contact in the bottom part where the polarization voltage is applied is evidenced in red. On the right part, the depletion process is shown: plotting the vertical field component under a contact along the depth of the detector, the increasing bias voltage start depleting the bulk from the top side until full depletion is achieved (-23 V).

Poisson law in the bulk of the material has been solved taking into account the bulk residual doping N_b:

$$\nabla^2 V(\vec{x}) = \frac{qN_b}{\varepsilon_0}\left[1 - exp\left(\frac{-qV(\vec{x})}{k_B T}\right)\right] \quad \text{Eq. (1.D.1)}$$

In addition to the above described boundary conditions, we also consider the possible formation of a surface charge with charge density N_S at the passivated gaps and on the lateral passivated surfaces. An example of calculated potential is reported in Fig. 1.D.1. The electric field *E* into the detector is then computed by doing the gradient and changing the sign.

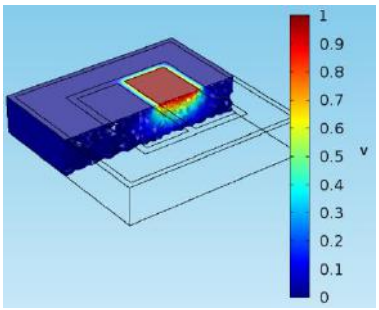

Figure 1.D.3: The weighting potentials for the first and second contacts.

The current signals produced by the detector after interaction with gamma particles are computed according to reference [14]. In details, we suppose that the gamma interaction produces point charges of hole and electron in a given place of the detector volume. Then the trajectory of holes and electrons are computed solving the following equation considering a minus sign for electrons and a plus for holes:

$$\dot{x_s}(t) = \mp \mu_s \vec{E}(\vec{x}_s(t)) \quad \text{Eq. (1.D.2)}$$

$$i_n(t) = \sum_{s=e,h} q_s \mu_s \vec{E}(\vec{x}_s(t)) \cdot \vec{E}_n(\vec{x}_s(t)) \quad \text{Eq. (1.D.3)}$$

$$Q_n(t) = \int_0^t i_n(\tau) d\tau \quad \text{Eq. (1.D.4)}$$

In order to use the obtained trajectories to compute the transient currents on the n contact (n = 1 or 2 in our case), the weighting potential is calculated by applying 1.0 V boundary condition at the considered contact and 0 elsewhere. The two weighting potentials are shown in Figure 1.D.3. Starting from the potential, weighting field are therefore computed along the trajectory.

Shockley-Ramo theorem [14] allows to calculate the transient current in each contact according to Eq. 1.D.3 and the induced charge is then calculated by simple integration (Eq. 1.D.4).

A theoretical data set of charge signals was calculated by the described numerical approach supposing interaction at different position into the detector. At the end of the next section (1.E) we will show a comparison between the signals obtained with these modelling and the experimental ones obtained in the laboratory with the segmented detector.

This model has also been used to calculate the possible effect of charge accumulation at passivated surface by computing the detector potential and the field line (that will correspond to the trajectory lines as well) at different charge surface density Ns. This result will be shown in section 1.F.

1.E. TEST OF THE SEGMENTED DETECTOR IN THE LABORATORY

The segmented detector described in section 1.B has been tested in the test cryostat described in section 1.C with a gap in between segments of 0.4 mm. In Figure 1.E.1 we can see in black squares the counting rate as function of the applied bias voltage (counting rate scale on the left) whereas the red circles shown the resolution for each applied voltage (FWHM scale on the right). Both segments have similar behavior: the counting rate increases with the applied voltage till a value near 18 V and then starts a plateau that means we have reach the depletion voltage. The measured resolution is nearly the same (near 0,7 keV) when the detector is fully depleted.

Figure 1.E.2 shows the spectra of ^{241}Am and ^{133}Ba up to 400 keV. Higher energies have very low efficiency because the reduce thickness of the detector (2mm).

Similar Figures can be seen for a similar detector with 0,2 mm gap.

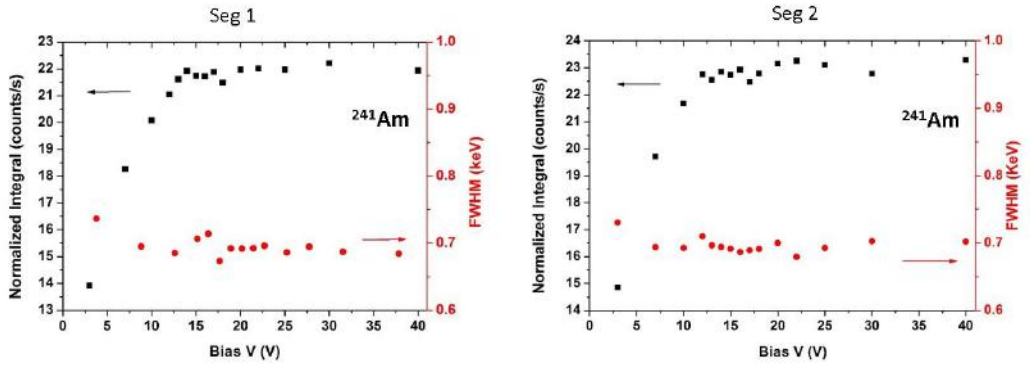

Figure 1.E.1: In black squares the counting rate as function of the applied bias voltage (counting rate scale on the left) whereas the red circles shown the resolution for each applied voltage (FWHM scale on the right). Both segments have similar behavior: the counting rate increases with the applied voltage till a value near 18 V and then starts a plateau that means we have reach the depletion voltage. The measured resolution is nearly the same for both segments, near 0,7 keV, after the detector is fully depleted.

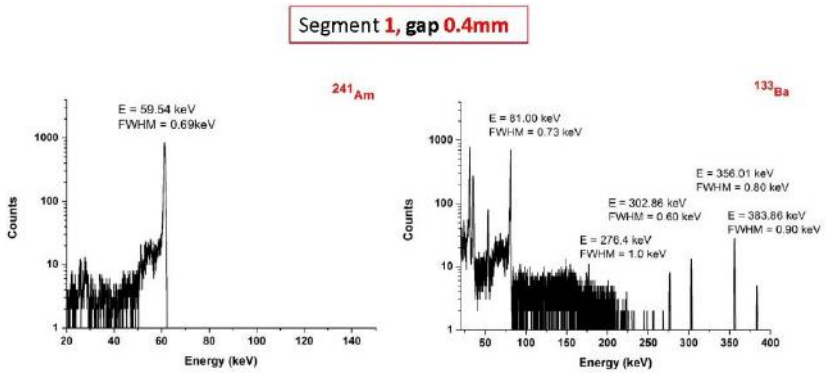

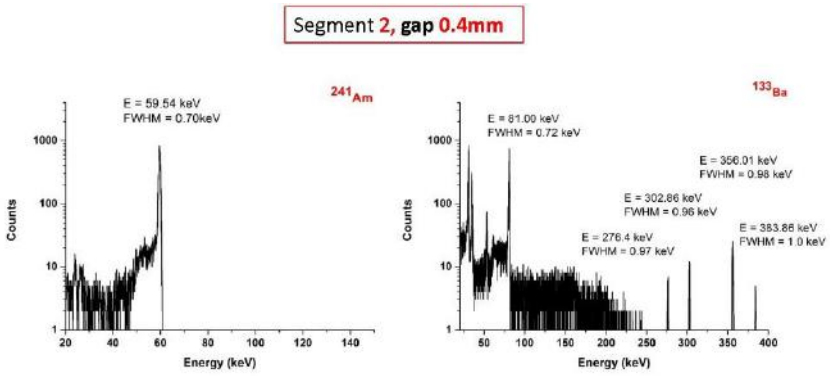

Figure 1.E.2 shows the spectra of ^{241}Am and ^{133}Ba up to 400 keV for both segments. Higher energies have very low efficiency because the reduce thickness of the detector (2mm). The gap in between segments is 0,4 mm.

In Figure 1.E.3 two experimental signals are compared with experimental ones. The higher signals correspond to the collecting contact the smaller oscillating ones correspond to the other contact: the first signal is typical of a net deposited charge due to a charge that enter the contact at the end of its trajectory, the second is a transient signal due to electrostatic induction on the contact not receiving the charge. The good agreement between the calculated and experimental signals can be obtained by moving selecting the position of the interaction from the calculated dataset. In particular, the two sets of signals are generated in the place indicated by the star symbols in the insets.

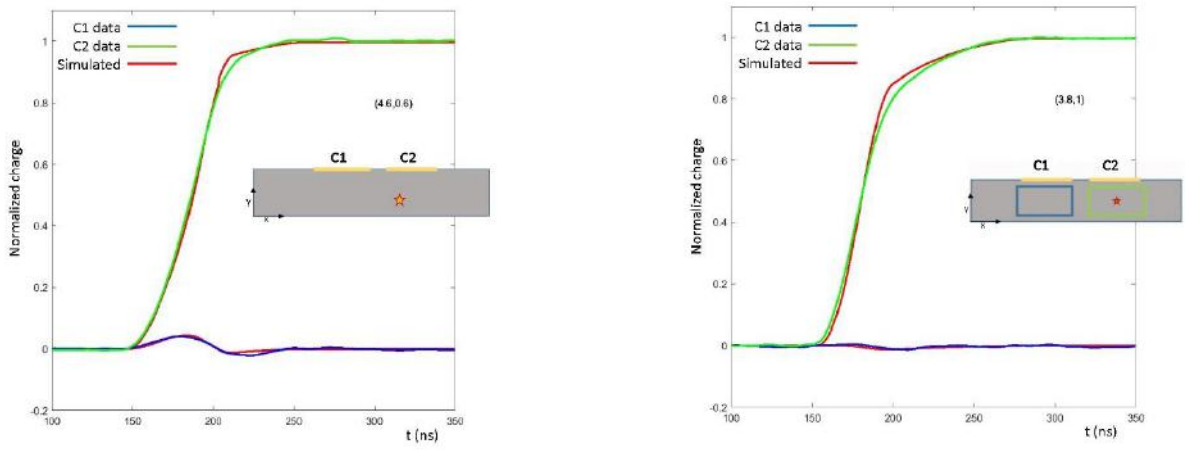

Figure 1.E.3: Both figures compare the signal shapes generated by COMSOL (red line) obtained in the modelling described in the precedent section 1.D with the real signals obtained with the segmented detector described in section 1.B.

1.F. MODELIZATION OF RESIDUAL CHARGE IN HPGE PASSIVATED SURFACES

With the model described in section 1.D we have studied the effects of the presence of a charge density in the passivation of the intrinsic Ge surfaces in between contacts, as described in section 1.A.
In Figure 1.F.1 are reported the results of the calculation for Ns (number of elementary charges by unit area)

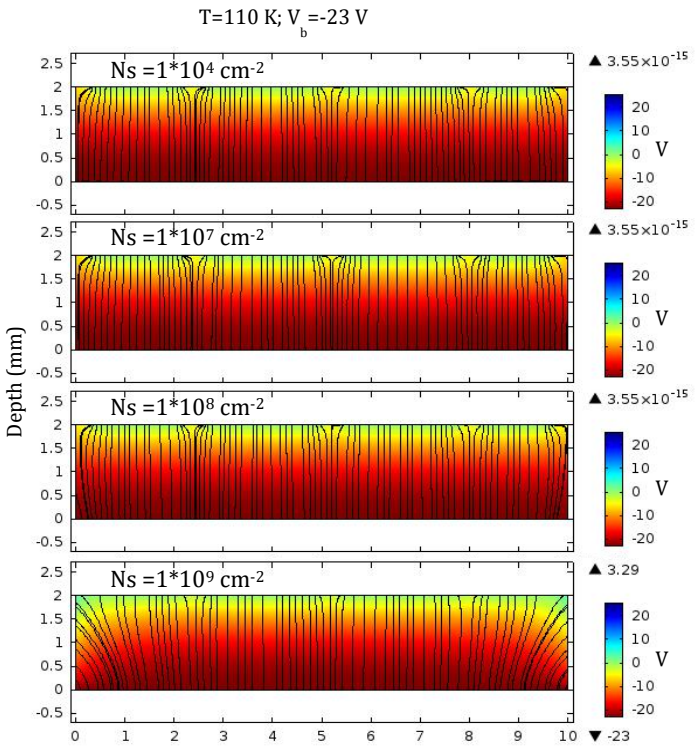

Figure 1.F.1: From top to bottom, bulk potential and field lines at increasing surface charge density Ns.

From 0 to 10^9 cm^{-2}. As can be see from 0 to 10^7 cm^{-2} elementary charge densities the filed lines patterns does not change meaning that passivation charge up to 10^7 cm^{-2} has negligible effect on the detector. At 10^8 cm^{-2} surface charge, field shape starts to change close to the border of the detector while at 10^9 cm^{-2} extended modification of the field lines are visible. In particular it can be seen that some lines finish to the lateral surface meaning that charges generated along that lines will be lost at the surface instead of producing a signal on the contact. This fact means that the volume of the detector where these lost lines are present can be interpreted as a dead volume as proposed in section 1.A.

It is worth to note that 10^9 cm^{-2} is not a huge amount of charge if we consider that the typical density of atoms at the surface (that is order of magnitude of the upper limit for charge traps surface density) is as much as 10^{15} cm^{-2}. This calculation can be very useful in order to analyze future measurements of dead volume into detector prototype in term of passivation charge density.

SECTION 2 - REPORT ON THE R&D ON NOVEL GE-DETECTOR GEOMETRIES FOR ULTIMATE POSITION RESOLUTION AND EFFICIENCY

The activity within the ENSAR2 PSeGe JRA of the GSI collaborators has focused on the development of semi-planar detector with point contacts as a segmentation tool. This includes a detailed study by numerical simulations of the electric field and the charge transport inside the detection crystal and a search for the optimal geometry. The main idea is to make several point read-outs on a planar crystal which are sensitive to certain area. The distribution and number of these points can be estimated by performing simulations taking the electric field and charge transportation into account. In this framework, a semi-planar HPGe detector with a single point contact read-out has been studied in order to characterize the behavior of such a novel contact technology replacing the segmentation of the crystal. A non-segmented p-type HPGe crystal with a dimension of 33.2x33.2x15.5 mm3 and Carrier concentration of 3.3x109 atom/cm3 was used for the test purposes. The crystal

which has an amorphous Ge (aGe) blocking contact with an efficient use of Ge material (see Figure 2.1) has a sensitive surface to low-energy radiation on contrary to the Li-diffused contact technology commonly used.

Figure 2.1: Quasi-planar prototype p-type HPGe detector with dimensions of 33.2x33.2x15.5 mm3 used in order to determine the energy resolution of such a system with a single point contact read out. The depletion voltage was calculated as 450V.

The assembly of the crystal was done at GSI by installing it into a POPTOP capsule as illustrated in Figure 2.2. The charge signal was extracted from the p+ electrode. The detector was operated at 100V and 1.2 pA leakage current was observed. Sudden increase of the leakage current when increasing the bias voltage caused the saturation of the preamplifier, which is related to the type of coupling used for the signal read-out. The detector was tested using ^{57}Co and ^{60}Co sources in order to cover the low and high-energy region. For each source, different shaping time constants were tested. Experimental data were fitted using an exponentially modified Gaussian function and the results for two different shaping time constants are given in Figure 2.5 for ^{57}Co and for ^{60}Co sources. The energy resolution values obtained for the defined cases are listed in Table 1. Using the ^{57}Co source, 2.1 keV and 2.3 keV energy resolution values at 122 keV line were obtained for 3 µs and 6 µs shaping time constants, respectively. While with the ^{60}Co source, 4.5 keV and 4.3 keV energy resolution values were obtained for the 1332 keV transition for 3 µs and 6 µs shaping time constants, respectively.

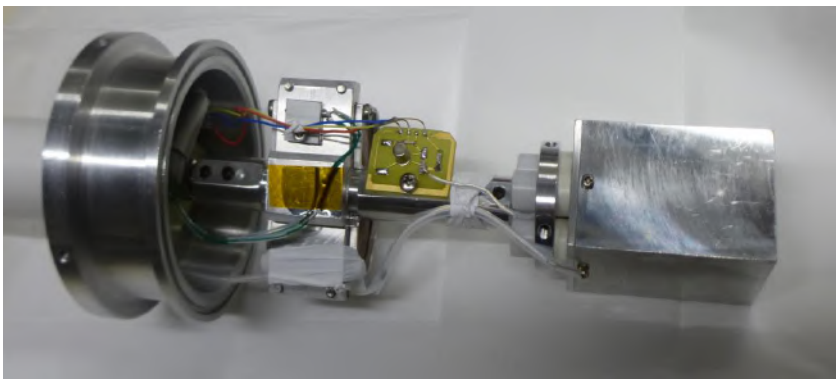

Figure 2.2: Semi-planar crystal placed in a POPTOP type capsule. The assembly and front-end electronics is shown.

The experimentally observed results were compared to the literature data obtained from the SEMIKON company where the crystal was bought. The verification tests were performed by using 241Am, 137Co sources and a pulser signal by SEMIKON. Additionally, the operation voltage was studied and defined as -480 V. Operating the detector

at -480 V, an energy resolution of 2.59 keV was achieved at 59.6 keV using a 241Am source and 2.55 keV with a pulser. The detector current at this operational voltage was 3 nA. The reason is assumed to be the different couplings that are used in two different systems. SEMIKON used AC coupling for the preamplifier, resulting in insensitivity of the gain potential from the detector current and higher operation voltage causing a larger depletion region, than used in the GSI measurement. The electronic drawings of these two different AC and DC couplings are shown in Figure 2.3 below.

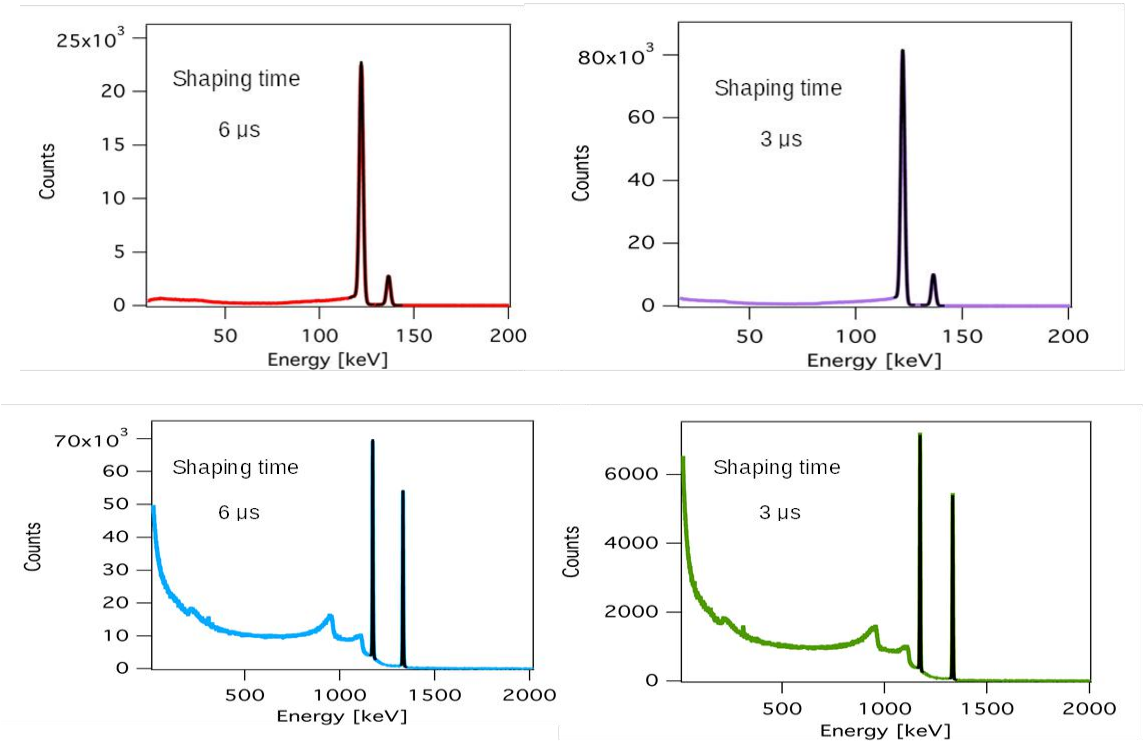

Figure 2.3: The observed energy spectrum with 57Co source. The spectrum on the left side was recorded using a 6 µs shaping time constant while the one on the right side was obtained with a 3 µs shaping time constant.

Table 2.1: Energy resolution values obtained with a semi-planar point-contact detector listed for 57Co and 60Co transitions, using different shaping time constants.

Shaping time (µs)	3	6
Energy (keV)	122	122
FWHM (keV)	2.13(1)	2.35(1)
Energy (keV)	1332	1332
FWHM (keV)	4.53(1)	4.32(1)

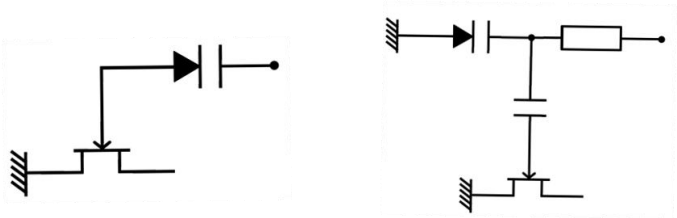

Figure 2.4: Different kind of couplings were used in order to read the signal at GSI and SEMIKON. Left drawing illustrates the DC coupling used at GSI and the left drawing shows the AC coupling used by SEMIKON.

Further tests of the detector have been performed, employing the original AC coupling, at the GSI 3D scanner table in order to determine the pulse shapes recorded from interactions occurring at different positions along the crystal. The focus of these tests was to study the effect of the field distribution on the pulse shapes as well the field defect sizes. The functioning of the GSI scanner is described in detail in reference [1]. The basic idea is to use a point-like 22Na β+ source to shine 511 keV -rays into a Ge detector with the associated second 511 keV -rays detected in a position sensitive scintillator detector. By operating both detectors in coincidence lines of interaction in the Ge detector are defined, such that multitudes of pulse shapes are measured along the lines. By performing a second measurement in perpendicular direction, a second band of lines with associated pulse shape multitudes is generated. Finally, a least-squares minimization technique enables to uniquely defines the pulse shape in any covered voxel of the Ge detector. Figure 2.5 shows the schematics of the scanner and depicts the measurement set-up.

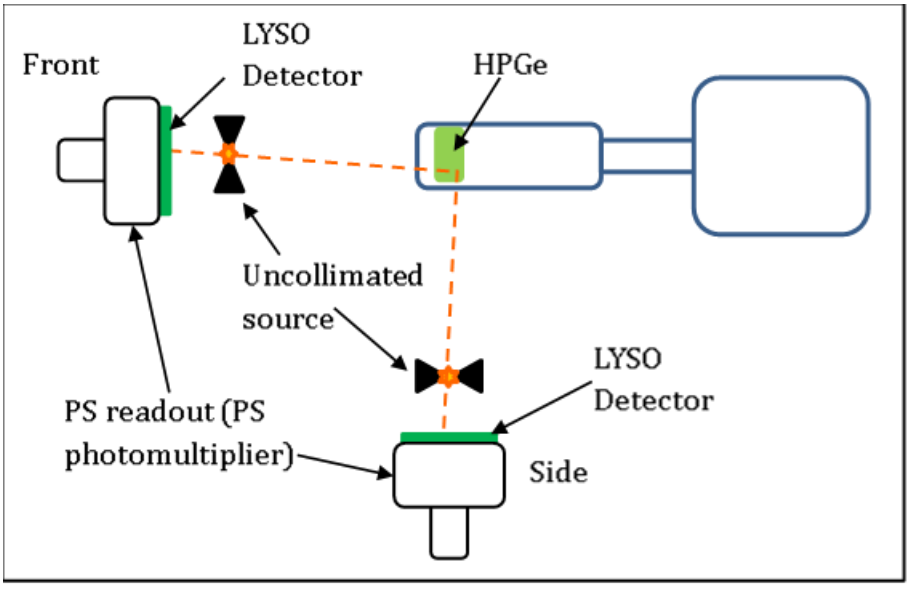

As shown in Figure 2.6 the scan revealed full depletion of the detector volume. Thus, the measured pulse shapes are characteristic for any detector position.

Figure 2.7 shows selected pulse shapes, indicating the expected variation as function of the position. The on-going analysis confirms the expected uniformity in the central region, while distinct deviations are observed towards the edges. Obviously, the detector has only small dead volume in the vicinity of the small groove at the backside. Thus, qualitatively the behavior predicted by previous modelling and simulation is proven. A quantitative comparison is on-going and is part of the continuation of the project beyond the time line of ENSAR2.

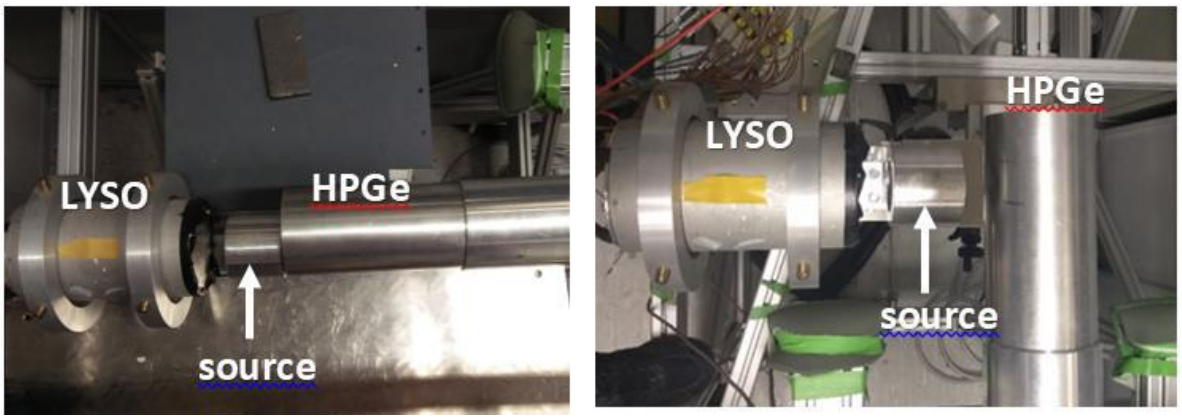

Figure 2.5: Schematics of the GSI scanner and the actual measurement set-up.

The current project was limited by the originally unexpected deterioration of the HPGe detector. Initially the noise behavior was expected. However, in the course of the project the noise level due to the leakage current increased continuously and reached a level that does not allow the planned segmentation of the two contacts. It is suspected that the grove guard ring is the origin of the leakage current as it has sufficient passivation. Therefore, it is planned to rebuild the prototype leaving the open surface as a step and reprocessing the contacts. By this way the field defect can be minimized, the reliability of the passivation enhanced and the active volume preserved.

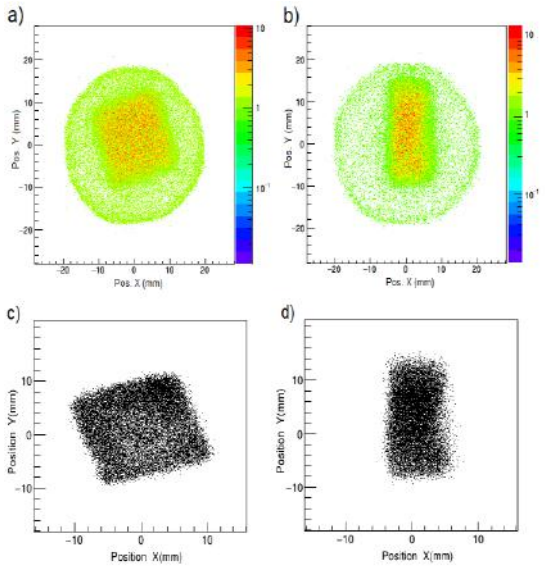

Figure 2.6: Images of the front (a, c) and side (b, d) scan.

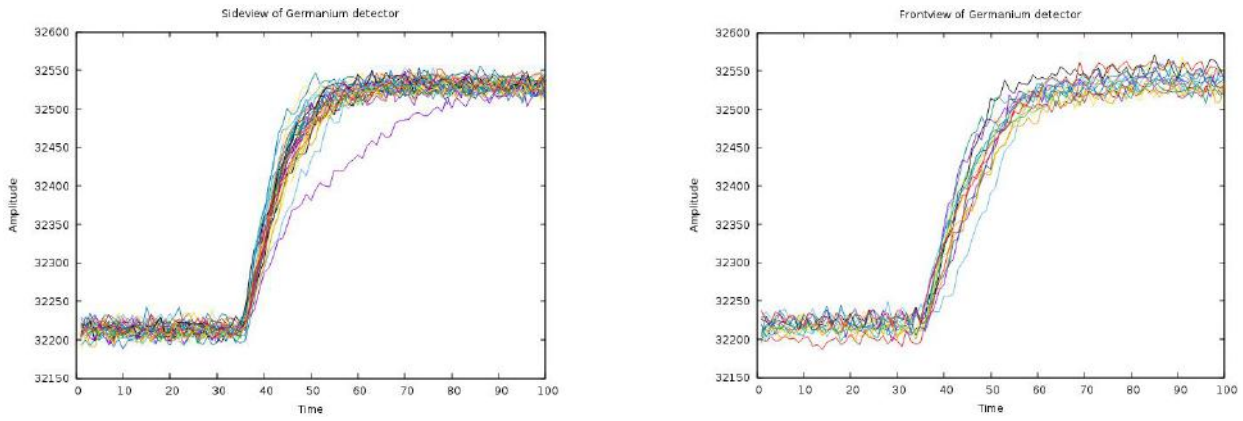

Figure 2.7: Multitudes of line shapes for the side and front scan of the Quasiplanar detector.

CONCLUSION

In this document we report on the advancement of Tasks 1 and 2 of the work package 10, the PSeGE JRA, within ENSAR2.

Regarding task 1, a strong collaboration, with INFN and the Padova University, IKP Cologne and IPHC Strasbourg as main actors, is working on segmentation and passivation techniques, test setup and on characterization of prototypes. The results with hydride passivation and Laser Thermal Annealing techniques for segmentation are very promising.

Regarding task 3, a detector prototype with the most promising geometry, the quasi-planar, that is expected to maximize both the position resolution and the detector active volume, has been produced and fully characterized. The results are very promising despite the instability of the prototype, that limited the possibility to perform further testing.